JOURNAL OF SOLID STATE CHEMISTRY 117, 392–397 (1995)

Phase Diagram of Nonstoichiometric 10 mol% Gd_2O_3-Doped Cerium Oxide Determined from Specific Heat Measurements

N. Stelzer and J. Nölting

Institut für Physikalische Chemie der Universität Göttingen, Tammannstrasse 6, 37077 Göttingen, Germany

and

I. Riess

Department of Physics, Technion I.I.T., Haifa 32000, Israel

Received September 15, 1994; in revised form December 20, 1994; accepted December 21, 1994

The phase diagram for nonstoichiometric 10 mol% Gd2O$_3$-doped cerium oxide, $Ce_{0.818}Gd_{0.182}O_{1.909-y}$, was determined from specific heat measurements in the temperature range 300–1250 K and composition range $Ce_{0.818}Gd_{0.182}O_{1.909}$–$Ce_{0.818}Gd_{0.182}O_{1.731}$, using a controlled diabatic scanning calorimeter. No phase transition was found in this temperature range for the composition $Ce_{0.818}Gd_{0.182}O_{1.909}$. The specific heat measurements reveal phase transitions for the composition range $Ce_{0.818}Gd_{0.182}O_{1.859}$–$Ce_{0.818}Gd_{0.182}O_{1.731}$. A phase diagram is constructed which shows a miscibility gap. The maximum of the miscibility gap occurs at the composition $Ce_{0.818}Gd_{0.182}O_{1.788}$ and T = 939 K. The phase diagrams of nonstoichiometric CeO_{2-x} and $Ce_{0.818}Gd_{0.182}O_{1.909-y}$ are compared and discussed in detail. © 1995 Academic Press, Inc.

1. INTRODUCTION

Over the past 2 decades cerium oxide, CeO_2, has been intensively investigated. Stoichiometric cerium dioxide adopts the fluorite structure. It can be doped with trivalent cations, such as gadolinium ions. These dopants substitute for the host cations and introduce oxygen-ion vacancies ($V_O^{\cdot\cdot}$) that provide charge compensation. The introduction of the trivalent Gd^{3+} ions produces one double-charged oxygen vacancy ($V_O^{\cdot\cdot}$) for every two Gd^{3+} ions. This can be described using Kröger-Vink notation:

$$Gd_2O_3 + 2Ce_{Ce}^{X} + O_O^{X} \leftrightarrow 2Gd'_{Ce} + V_O^{\cdot\cdot} + 2CeO_2. \quad [1]$$

In undoped and reduced ceria, CeO_{2-x}, the vacancies order at low temperature to form a superlattice (1–9). Therefore only a few discrete CeO_y nonstoichiometric phases exist at low temperatures ($T < 722$ K); see Fig. 1. We examine here doped and reduced CeO_2. It is the purpose of the present work to discuss in detail the phase diagram of nonstoichiometric 10 mol% Gd_2O_3-doped CeO_2 ($Ce_{0.818}Gd_{0.182}O_{1.909-y}$) in comparison with CeO_{2-x}. We used 10 mol% Gd_2O_3-doped CeO_2 because it has high ionic conductivity and low activation energy (10), favoring it for possible industrial applications (11). The structure of this composition is expected to be roughly that of the composition with 25% Gd^{3+} cations, which we therefore take as a reference model. For this model one possible periodic arrangement of Gd^{3+} is at the corner of the fcc unit cell. In this case, it is easy to show that, for the average arrangement, $V_O^{\cdot\cdot}$ is not a nearest neighbor of two Gd^{3+} cations, because they are too far apart. On the other hand we have to take into account that, due to the fluctuations in the Gd^{3+} distribution, some Gd^{3+} could form closer pairs to which a single $V_O^{\cdot\cdot}$ is the nearest neighbor. It is not clear a priori if the Gd^{3+} impurities are randomly distributed as assumed, for example, by Nowick (12), or are ordered so as to form a maximum number of bonds with $V_O^{\cdot\cdot}$, i.e., forming closer pairs which share $V_O^{\cdot\cdot}$. Neglecting kinetic limitations, then, the answer depends on the temperature, according to the requirement that the free Gibbs energy ($G = H - TS$) is minimized. Therefore at high T, disorder is preferred, even if the binding energy of $(Gd'_{Ce}–V_O^{\cdot\cdot})^{\cdot}$ is larger than the repulsion energy between two close (Gd'_{Ce}–Gd'_{Ce}) compared to two more remote ones. Thus at the high temperature of preparation of the oxide (~1873 K), one expects that Gd is randomly distributed. At lower temperature (~1273 K) if the formation of Gd'_{Ce} pairs bound to $V_O^{\cdot\cdot}$ is preferred, it may take place even if the diffusion of Gd in CeO_2 is low, since the rearrangement needed is only over a unit cell distance. However, the fact that in unreduced Gd-doped CeO_2 the vacancies $V_O^{\cdot\cdot}$ are mobile at $T \sim 1273$ K suggests that the binding energy to form $2Gd'_{Ce} - V_O^{\cdot\cdot}$ is too low to enforce the formation of these complexes at that temperature.

0022-4596/95 $12.00

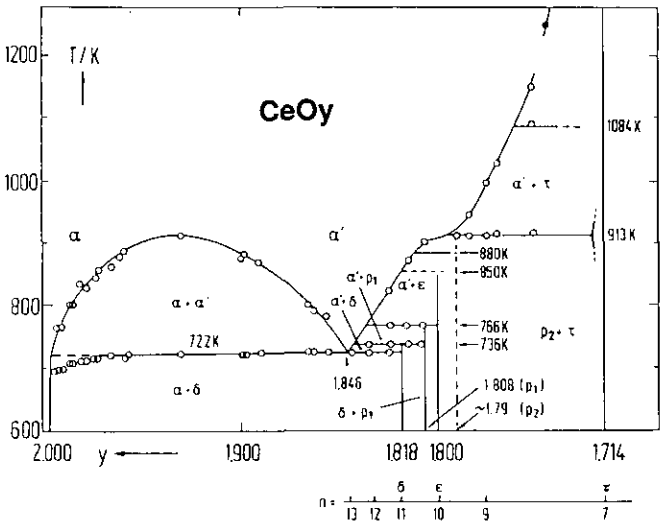

FIG. 1. The phase diagram of CeO_{2-y} in the composition range CeO_2–$CeO_{1.714}$ and $600 < T < 1300$ K from Ref. (7). One data point (●) is added from Ref. (22).

Therefore, Gd'_{Ce} is likely to be randomly distributed at $T \sim 1273$ K. The increase in the activation energy for concentrations larger than 18% Gd^{3+} cations is believed to be a result of the formation of a low concentration of pairs of Gd–Gd due to spatial fluctuations, causing a binding of $V_O^{\cdot\cdot}$ (10).

Doped cerium oxide is reduced at elevated temperatures and low oxygen pressures, increasing the concentration of $V_O^{\cdot\cdot}$. New phases are found if the oxygen vacancies $V_O^{\cdot\cdot}$ can order. The former question of the ordering of Gd is also of importance when dealing with possible phases obtained by reduction. If Gd'_{Ce} is immobile, this is expected to eliminate many of the possible ordered distributions of $V_O^{\cdot\cdot}$. On the other hand, three-dimensional ordering of Gd'_{Ce} requires a motion on the atomic scale only, which may take place even if the diffusion coefficient $\tilde{D}_{Gd}$ is very low. The driving force for this motion could be an increased binding energy for $(Gd'_{Ce}$–$V_O^{\cdot\cdot})$ in the ordered state. Therefore, phases with 3-D ordered Gd and $V_O^{\cdot\cdot}$ may exist.

The point of reference for a comparison with CeO_{2-x} is the composition before reduction. Experimentally it is the one obtained at ~1 bar O_2, which is assumed not to be reduced. This composition is then $Ce_{0.818}Gd_{0.182}O_{1.909}$. The reduced oxides are $Ce_{0.818}Gd_{0.182}O_{1.909-y}$. They are compared with CeO_{2-y}.

2. EXPERIMENTAL

2.1. General

The instrument used for the measurement of specific heat is a controlled diabatically shielded temperature scanning calorimeter. The diabatic method is based on a precisely controlled heat loss between the sample and the surrounding shield. The calorimeter is built quite similarly to an adiabatic one. Losses are induced by keeping the heat shield around the sample holder at a temperature a few degrees celcius lower than the sample holder. The power needed to maintain a fixed temperature is measured. It equals the heat loss at that temperature. By introducing the heat loss, measurements can be done not only on heating but also on cooling. Further details can be found in Ref. (13, 14). The procedure has two significant advantages over the adiabatic calorimetric methods normally used:

(a) The adverse effects of uncontrolled heat transfer to the surroundings are eliminated. For example, altering thermocouples or changing emissivities of the surrounding walls have no apparent influence on the heat balance of the sample, as the actual heat loss is being measured and taken into consideration.

(b) The input heat to the sample can be varied within a certain range to allow also the lowering of the temperature by supplying less heat than is being lost. Hence, calorimetric measurements with decreasing temperature are possible with scanning rates limited only by the probe-shield heat loss flux.

The experimental setup (see Fig. 2) allows *in situ* changes in the oxygen content of the sample by introduction of a gas mixture of H_2/H_2O. A molybdenum sample

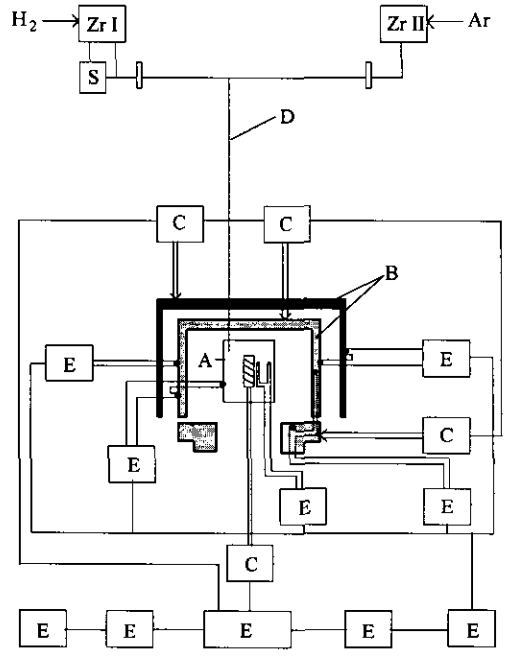

FIG. 2. Schematics of specific heat measuring setup. (A) sample holder, (B) shieldings, (C) heating elements, (D) gas handling system, (E) measurement and control electronics.

holder is constructed which enables the sample to be flushed by controlled gases. The gas system allows the flushing of the sample and/or calorimeter either with oxygen-free Ar ($P_{O_2} \leq 10^{-19}$ bar) or with H_2/H_2O mixtures.

2.2. Sample Holder

A molybdenum sample holder is used because it has a relatively low specific heat (15), has no phase transitions in the relevant temperature range, and shows high chemical resistance for the oxide and gases used. It has a cylindrical shape (37 mm length, 32 mm diameter) with a central bore (A) for the inner heater. Figure 3 shows a section. Four cylindrical holes (13 mm diameter) are arranged around the heater to accommodate the pressed cylindrically shaped samples. The holes are closed, gas-tight, by four molybdenum covers. Two thin molybdenum capillaries (C) at the edge of the sample holder are connected to the four inner probe holes by perpendicular channels which serve as the inlets and outlets for the gases. The large holes for the probes are interconnected by small bores (S) to achieve the proper distribution of the flushing gas all over the probe material.

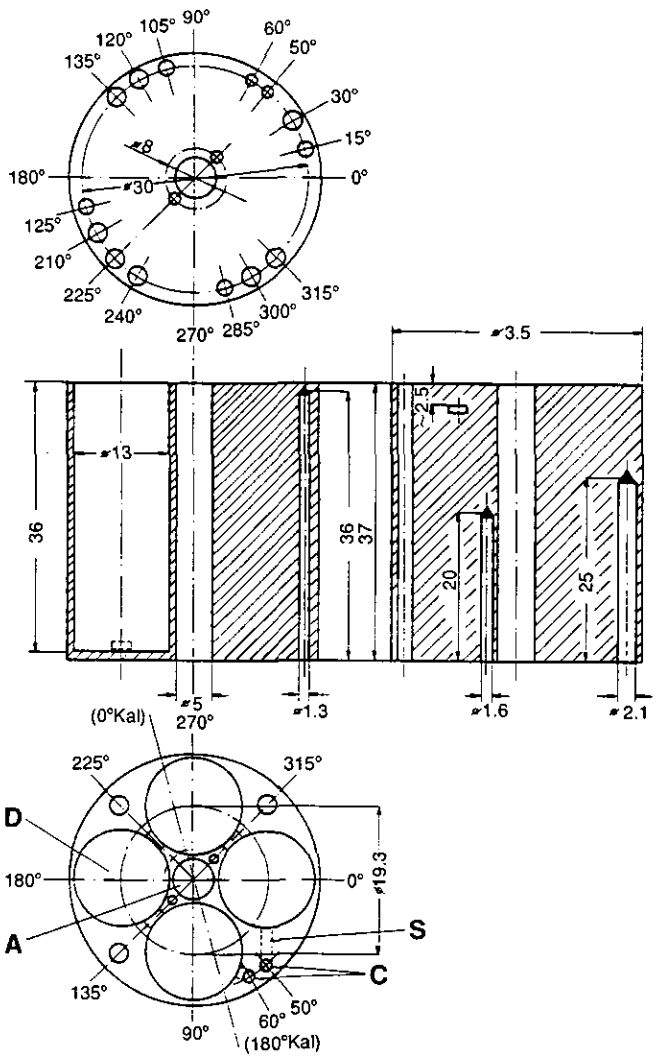

FIG. 3. Sections of the sample holder. (A) central bore for the inner heater, (C) thin capillaries for the in- and outgoing gas, (D) cylindrical holes for the samples, (S) channel for distributing the incoming gas.

2.3. Sample Preparation

A fine-grained powder of the mixed oxide $Ce_{0.818}Gd_{0.182}O_{1.909}$ was prepared by coprecipitation of the corresponding oxalates followed by calcination. The powder was tumbled in a ball mill, pressed at 900 MPa into cylindrical pellets (12 mm diameter), and sintered for 1.5 hr at 1273 K. The reader is referred to Ref. (16) for a detailed description of the sample preparation.

2.4. Gas System

An H_2/H_2O mixture was used to reduce the sample. The sample was then flushed by oxygen-free Ar. The rest of the calorimeter was constantly flushed with pure Ar to protect the inside of calorimeter from oxygen to keep the sample in a reduced state. Ar and H_2 were purified from oxygen by porous zirconium metal held at 1173 K. The rate of flow of the gases varied between 0.5 and 1 cm^3 per sec. At the end of the gas system the oxygen partial pressure of the actual outcoming gas or gas mixture was monitored using a calcium-stabilized zirconium solid state electrochemical cell. P_{O_2} there did not exceed 10^{-19} bar.

2.5. Sample Handling

The reduction of the mixed oxide $Ce_{0.818}Gd_{0.182}O_{1.909-y}$ was carried out *in situ* by flushing the sample with a defined H_2/H_2O gas mixture, followed by equilibration under purified argon. The oxygen partial pressure of the H_2/H_2O mixtures was controlled by the temperature of the saturator (273–294 K) and the temperature of the sample (900–1250 K). The typical time of reduction and equilibration was 24 hr. The equilibration was carried out until P_{O_2} at the outgoing H_2/H_2O gas mixture reached a steady level. At the end of this procedure the sample was assumed to be homogeneous. For the specific heat measurements, the calorimeter was flushed with purified argon ($P_{O_2} \leq 10^{-19}$ bar) to protect the reduced sample, to ensure that the state of reduction remained practically constant while the temperature varied between room temperature and 1250 K. When the reduction temperature, T_R, ($900 \leq T_R \leq 1250$ K) was below 1250 K, a small amount of oxygen was liberated into the flowing Ar at T above T_R. However, this occurred at very low P_{O_2} and the amount of oxygen liberated was negligible.

2.6. *Measurement Procedure*

At the beginning of the experiment the heat capacity of the empty sample holder was determined. The specific heat of the sample was determined by subtracting this value from the measured heat capacity of the filled sample holder. The so-called stoichiometric (i.e., chemically balanced) $Ce_{0.818}Gd_{0.182}O_{1.909}$ was introduced into the molybdenum sample holder and closed. The sample holder, including the sample, was weighed. The sample was then introduced into the calorimeter and reduced as discussed before. The controlled diabatic C_P measurements were then performed between 300 and 1250 K at a heating rate of 0.4 or 0.8 K per min. We observed no marked differences in the results for the two heating rates. C_P measurements with decreasing temperatures were conducted between 1250 and 600 K at a cooling rate of 0.4 K per min. This procedure of measuring C_P on heating and subsequently on cooling in one experiment was repeated for each state of reduction. At the end of the C_P measurements for a fixed state of reduction, the sample holder was taken out of the calorimeter and weighed so that changes in the oxygen content of the sample could be determined. Taking the small openings ((C) in Fig. 3) of the sample holder into account, the rate of oxidation at room temperature is low and oxidation of the sample is slow. This allowed us to determine y with an accuracy of $\pm 5 \times 10^{-4}$. The procedure of reduction and subsequent C_P measurements was then repeated in the composition range $1.909 \geq y \geq 1.731$.

The temperature and the heating power were monitored every 3 sec with high precision. The sensitivity of measuring C_P values was better than 0.1 $J \cdot mol^{-1} \cdot K^{-1}$. The C_P values were calculated every 2 K. The transition temperatures could be measured within ±0.2 K. They differ slightly on heating and cooling as is shown below.

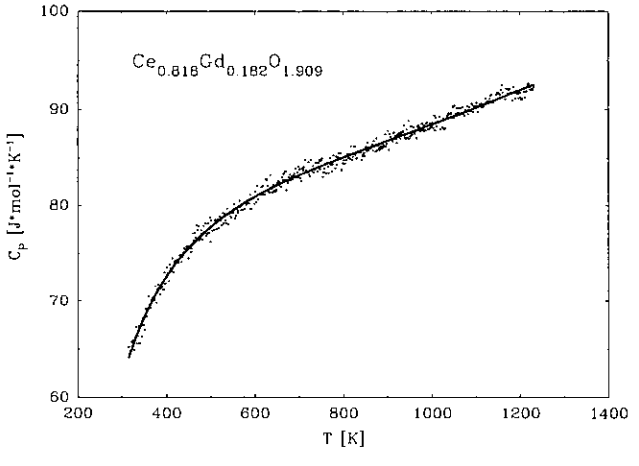

FIG. 4. Specific heat of $Ce_{0.818}Gd_{0.182}O_{1.909}$. (●) measured data, (—) best fit of theoretical curve.

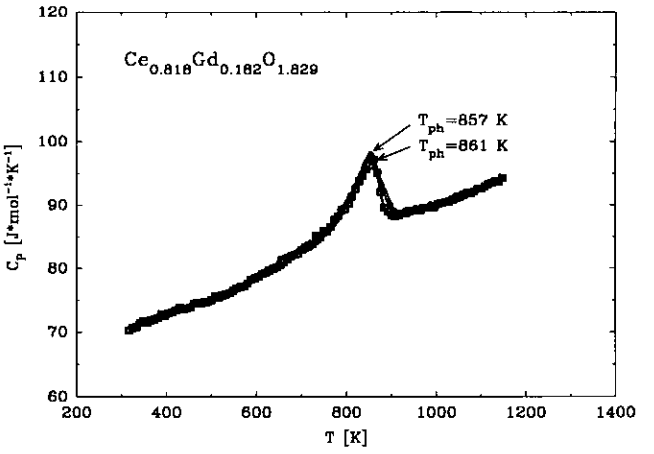

FIG. 5. Specific heat of $Ce_{0.818}Gd_{0.182}O_{1.829}$ during (□) heating and (●) cooling measurements.

3. RESULTS

3.1. *Specific Heat*

The stoichiometric $Ce_{0.818}Gd_{0.182}O_{1.909}$ exhibits no phase transition in the investigated temperature range. The C_P values for $Ce_{0.818}Gd_{0.182}O_{1.909}$ are shown in Fig. 4. The analysis of $C_P(T)$ is given elsewhere (14, 17).

As an example for a reduced sample, the specific heat

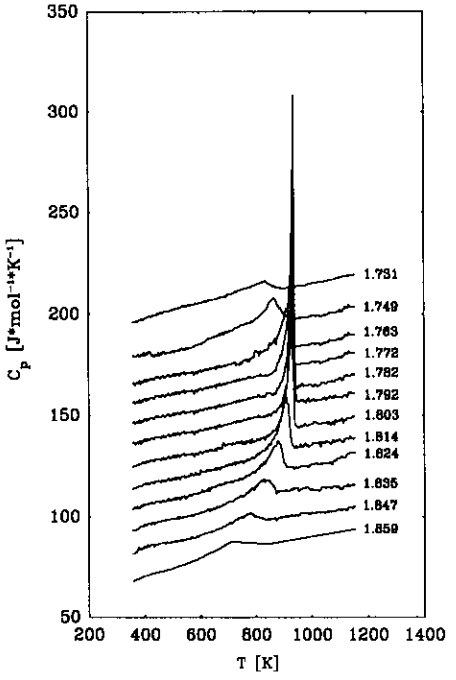

FIG. 6. Specific heat on heating of $Ce_{0.818}Gd_{0.182}O_{1.909-y}$ from $Ce_{0.818}Gd_{0.182}O_{1.859}$ to $Ce_{0.818}Gd_{0.182}O_{1.731}$. The curves are displaced in the vertical direction. The displacement between the curve with $x = 1.859$ and curves with $x < 1.859$ was calculated by taking the oxygen content into consideration, as given in the example: $1000 \cdot (1.859 - 1.847) = 12$. So the measured specific heat of $Ce_{0.818}Gd_{0.182}O_{1.847}$ was shifted by 12 $J \cdot mol^{-1} \cdot K^{-1}$.

for the sample with the composition $Ce_{0.818}Gd_{0.182}O_{1.829}$ is shown in Fig. 5. It exhibits a shoulder with a maximum value at 861 K for heating and 857 K for cooling measurements. This shoulder indicates a gradual transformation between two phases (6, 7). A set of C_P measurements for various nonstoichiometric $Ce_{0.818}Gd_{0.182}O_{1.909-y}$ is presented in Fig. 6. A variation of the transition temperatures with the composition is clearly observed. This information is used to construct the phase diagram shown in Fig. 7. In this phase diagram the curves were drawn through points determined by the maxima of the shoulders in C_P measurements taken under both heating and cooling.

We note a difference of 4 K in the transition temperature between heating and cooling for all reduced samples. In comparison, in determining the phase diagram of nonstoichiometric CeO_{2-y}, differences of ~15 K in the transition temperature between heating and cooling were observed in C_P measurements (18) as well as in dilatometer measurements (19). At the boundary of the miscibility gap, a transition of ($\alpha \rightarrow \alpha'$) or ($\alpha' \rightarrow \alpha$) occurs (see Figs. 1 and 7). The small difference in the transition temperature on heating and cooling may indicate a high similarity in partial volume of the two phases α and α'. The miscibility gaps of $Ce_{0.818}Gd_{0.182}O_{1.909-y}$ and CeO_{2-y} are compared in Fig. 8.

3.2. *Enthalpy of Transformation*

The calorimetric measurements enable quantitative calculations of the enthalpy change in the sample at constant composition. The determined enthalpies of transformation at the miscibility gap boundary for the composition range $Gd_{0.818}Ce_{0.182}O_{1.859}$–$Gd_{0.818}Ce_{0.182}O_{1.731}$ during heating and cooling are shown in Fig. 9. The maximum of the enthalpy of transformation is obtained for the composition $Ce_{0.818}Gd_{0.182}O_{1.788}$. The differences in the enthalpies of transformation between heating and cooling are very small, as shown in Fig. 9. The two-phase transformation at the miscibility gap boundary is different from that of a eutectic or peritectic phase transition. This is discussed in detail in Ref. (7).

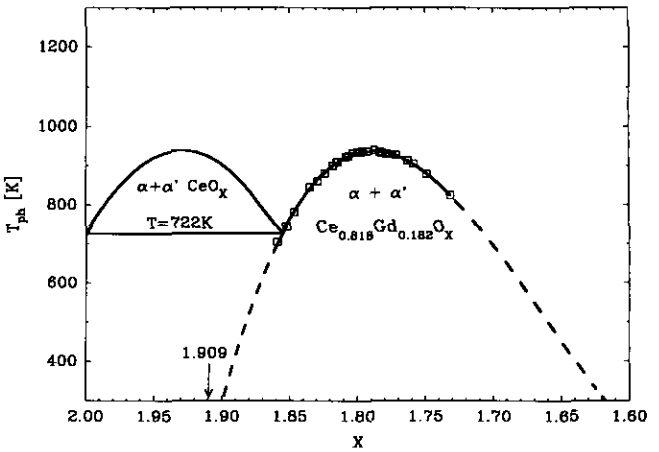

FIG. 8. Comparison between the miscibility gaps of $Ce_{0.818}Gd_{0.182}O_{1.909-y}$ and CeO_{2-y}.

4. DISCUSSION

The undoped oxide CeO_x can be reduced from CeO_2 to $CeO_{1.5}$. The α phase at $T < 722$ K (see Figs. 1 and 8) has a narrow range of existence close to CeO_2. Above 722 K the α phase broadens and exists between CeO_2 and $CeO_{1.93}$ at the temperature 921 K of the maximum of the miscibility gap of CeO_x. At $T < 722$ K a series of phases are observed in the composition range CeO_2–$CeO_{1.714}$. Comparison of Figs. 7 and 8 shows that the phase diagram of $Ce_{0.818}Gd_{0.182}O_x$ is quite different.

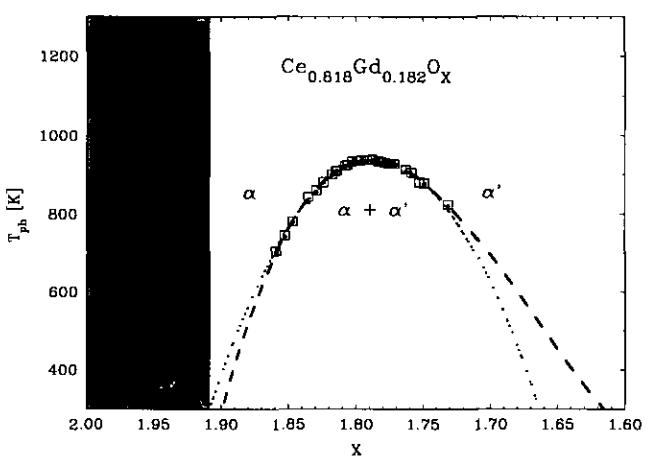

FIG. 7. Phase diagram of $Ce_{0.818}Gd_{0.182}O_{1.909-y}$. (□) from C_p measurements taken on heating and (●) on cooling. (...) parabolic extrapolation, (---) cubic extrapolation.

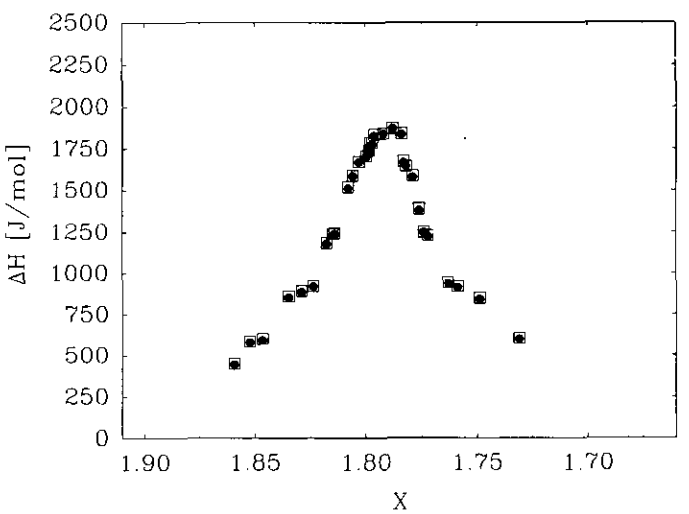

FIG. 9. Enthalpies of transformation near the miscibility gap boundary from $Ce_{0.818}Gd_{0.182}O_{1.859}$ to $Ce_{0.818}Gd_{0.182}O_{1.731}$.

(a) The boundary of the α phase is at $x = 1.909$. Maximum reduction is expected to occur at $Ce_{0.818}Gd_{0.182}O_{1.5}$; thus the range over which the oxygen content can be varied is reduced from $2 - 1.5 = 0.5$ for CeO_x to $1.909 - 1.5 = 0.409$ for $Ce_{0.818}Gd_{0.182}O_x$.

(b) No eutectic phase transitions are observed above room temperature for $1.909 \geq X \geq 1.731$. Only a miscibility gap is observed. Assuming that equilibrium prevails, this result indicates that the transition temperatures of the miscibility gap or a possible eutectic phase lies below room temperature. As a consequence no nonstoichiometric phases are detected by the C_p measurements in the composition range $Ce_{0.818}Gd_{0.182}O_{1.909}$–$Ce_{0.818}Gd_{0.182}O_{1.731}$. This is in agreement with results of conductivity measurements of Pascual (20, 21) and X-ray diffraction measurements of Faber *et al.* (10).

(c) The fact that the differences in C_p measured on heating and cooling are small is consistent with the claim that the phase transitions occur below room temperature.

(d) The elimination of reduced phases can be due to weakening of the effective $V_O^{\cdot\cdot}$–$V_O^{\cdot\cdot}$ interaction in the doped material. It can also originate from the fact that Gd is randomly distributed and frozen. As Gd'_{Ce} may bind $V_O^{\cdot\cdot}$ at low T it can prohibit the oxygen vacancies $V_O^{\cdot\cdot}$ from ordering in a three-dimensional superlattice.

(e) The α phase at temperatures above the miscibility gap ($T > 939$ K) is observed down to at least $x = 1.731$, while in CeO_x (see Fig. 1) it extends only down to $x \sim 1.8$ for $T \sim 940$ K at the boundary of the $(\alpha' + \tau)$-region.

(f) The miscibility gap in $Ce_{0.818}Gd_{0.182}O_x$ is much wider than in CeO_x. However, the temperatures at the maximum are similar (939 K on heating (935 K on cooling) vs 921 K, respectively) and the width at comparable high temperatures is also similar. This indicates that the high-temperature properties of the α phase are dominated by the oxygen vacancies in excess of those in the stoichiometric composition.

(g) The α phase exists at least down to 1.909 at room temperature and down to 1.788 at 939 K. The fact that at low T the α phase does not exhibit a large deficiency of oxygen below the chemically balanced value shows that the gain in energy due to a possible binding of Gd'_{Ce} with $V_O^{\cdot\cdot}$ to form excess $(Gd'_{Ce}–V_O^{\cdot\cdot})^{\bullet}$ pairs is not sufficient to allow reduction.

(h) The fact that no peak is seen in C_p for $x > 1.859$ suggests that the α phase boundary is steeper than in the parabolic extrapolation (dotted line in Fig. 7) e.g., along the dashed line, and that a small but finite reduction of $y \approx 0.01$ is possible in the α phase at room temperature.

REFERENCES

1. G. Brauer and K. Gingerich, *in* "Rare Earth Research Lake Arrowhead Ca. 1960" (E. V. Kleber, Ed.), p. 96. Macmillan, New York, 1961.
2. D. J. M. Bevan and J. Kordis, *J. Inorg. Nucl. Chem.* **26,** 1509 (1964).
3. D. J. M. Bevan, *J. Inorg. Nucl. Chem.* **1,** 49 (1955).
4. H. T. Anderson and B. J. Wuensch, *in* "Fast Ion Transport in Solids" (W. van Gool, Ed.), p. 284. North-Holland, Amsterdam, 1973.
5. S. P. Ray, A. S. Nowick, and D. E. Cox, *J. Solid State Chem.* **15,** 344 (1975).
6. M. Ricken, J. Nölting, and I. Riess, *J. Solid State Chem.* **54,** 89 (1984).
7. I. Riess, M. Ricken, and J. Nölting, *J. Solid State Chem.* **57,** 314 (1985).
8. L. Eyring, *in* "Nonstoichiometric Oxides" (O. Toft Soerensen, Ed.), p. 338. Academic Press, New York, 1981.
9. J. S. Anderson, *J. Phys. C* **38,** (1977).
10. J. Faber, C. Geoffroy, A. Roux, A. Sylvestre, and P. Abe'lard, *Appl. Phys. A* **49,** 225 (1989).
11. M. J. Murray and S. P. S. Badwal, *in* "Ceramic Developments, Materials Science Forum" (C. C. Sorrell and B. Ben-Nissan, Eds.), Vol. 34–36, pp. 213. Trans. Tech. Pubs. Switzerland, 1988.
12. A. S. Nowick, *J. Phys. Chem. Solids* **48,** 563 (1987).
13. J. Nölting, *Thermochim. Acta* **94,** 1 (1985).
14. N. Stelzer, "Thermodynamische Untersuchungen am System Cer-Gadolinium Sauerstoff (-Kalorimetrische und elektrochemische Methoden-)," Cuvillier Verlag, Göttingen, 1993.
15. R. C. Weast, (Ed.), "Handbook of Chemistry and Physics," 64th ed. CRC Press, Boca Raton, FL, 1983–1984.
16. A. Overs and I. Riess, *J. Am. Ceram. Soc.* **65,** 606 (1982).
17. N. Stelzer, J. Nölting, I. Riess, to appear.
18. S. Haftka, Thesis, Göttingen University, 1987.
19. R. Körner, M. Ricken, J. Nölting, and I. Riess, *J. Solid State Chem.* **78,** 136 (1989).
20. C. Pascual, *Sci. Ceram.* **12,** 729 (1984).
21. C. Pascual, Thesis, Madrid University, 1980.
22. J. Campserveux and P. Gerdanian, *J. Solid State Chem.* **23,** 73 (1978).